out of phase can be readily constructed as $P_2 - P_3$ and $2P_1 - P_2 - P_3$.

In summary, it has been shown that four parameters are required to characterize the power transfer properties of the lossless 3 X 3 coupler. These parameters can be obtained from splitting ratio data. It has further been shown how the performance of a fiber interferometer incorporating a 3 X 3 coupler can be predicted from these parameters.

References

[1] S. K. Sheem, "Optical fiber interferometers with [3 X 3] directional couplers: Analysis," *J. Appl. Phys.*, vol. 52, pp. 3865-3872, 1981.

[2] W. H. Glenn, "Investigation of techniques for the detection of small phase shifts in optical fibers," United Technologies Research Center, East Hartford, CT, Rep. R79-924576-1, 1979; also A. Dandridge, A. B. Tventen, and T. G. Giallorenzi, "Homodyne demodulation scheme for fiber optic sensor using phase generated carrier," *IEEE J. Quantum Electron.*, this issue pp. 1635-1641.

[3] R.M.A. Azzam and N. M. Bashara, *Ellipsometry and Polarized Light.* Amsterdam: North-Holland, 1977, p. 24.

[4] S. Lang, *Linear Algebra.* Reading, MA: Addison-Wesley, 1966, ch. 3.

[5] Changing the location of the reference points for the couplers has the effect of adding a constant to ϕ. Since such a constant does not change the relative phase between P_1, P_2, and P_3 (14); it is unimportant.

[6] M. Born and E. Wolf, *Principles of Optics.* Oxford: Pergamon Press, 1980, ch. 1.

Richard G. Priest, for a photograph and a biography, see p. 511 of the April 1982 issue of this TRANSACTIONS.

2 × 2 Optical Waveguide Matrix Switch Using Nematic Liquid Crystal

MORIO KOBAYASHI, HIROSHI TERUI, MASAO KAWACHI, AND JUICHI NODA

Abstract—**A 2 X 2 nonblocking optical matrix switch, composed of four elemental switches formed in a slab waveguide, is described. Switching action is based on total internal reflection caused by an electrically controlled change in refractive index of the liquid crystal. Propagation loss was remarkably reduced to 2.3 dB/cm, both by using liquid crystal as a cladding layer and by operating at the 1.31 μm wavelength. The experimental matrix switch exhibited 7.3-7.7 dB insertion loss, -17.3 to -18.2 dB crosstalk, and a 14° switching angle.**

I. Introduction

OPTICAL switches play an important role in optical communication systems. Especially, matrix switches are indispensable for exchanging optical information signals in local offices. Several bulk and waveguide matrix switches have been studied so far [1]-[9]. The bulk mechanical matrix switch using movable prisms exhibited excellent characteristics such as low insertion loss and low crosstalk [1], [2]. However, the bulk matrix switch has limitations in production, compactness, and speed. Waveguide matrix switches are expected to be superior to the bulk matrix switch in performance, such as in alignment free structure, easy integration of a large number of elemental switches on a common substrate, and speed. Waveguide matrix switches are classified into the following two types: nonblocking switches based on total internal reflection [3]-[6]; and blocking switches based on total internal reflection [7] or a directional coupler [8]. The nonblocking matrix switch is a more suitable switch for switching networks in local offices than a blocking matrix switch because the nonblocking matrix switch can accomplish input-output connection upon request by actuating independently only one elemental switch corresponding to the input and output ports. A nonblocking total internal reflection matrix switch using mechanically moving *GGG* chips exhibited a large switching angle of 22°, which is very useful for constructing the matrix switch [3]. However, the use of the moving *GGG* chips restricts the realization of a large scale matrix switch because it is difficult to compactly arrange the *GGG* chips in a matrix fashion. The nonblocking total internal reflection matrix switch using the $LiNbO_3$ waveguide is advantageous for switching times up to nanosecond. However, it is difficult to integrate a large number of elemental switches because of the small switching angle of less than 4°. The small switching angle arises from a small refractive index change, induced by an external electric field in $LiNbO_3$.

It is well known that the refractive index change in nematic liquid crystal is orders of magnitude larger than that in $LiNbO_3$. The large refractive index change in liquid crystal is convenient for constructing a compact matrix switch. Recently, a bulk nonblocking 4 X 4 matrix switch using nematic liquid crystal has been developed [9]. Although a waveguide switch using nematic liquid crystal has also been reported, it cannot be applied to the matrix switch because of the "on-off" switching action [10].

This paper describes an electrically controlled nonblocking waveguide matrix switch, based on total internal reflection, which is composed of a SiO_2-Ta_2O_5 waveguide film and a nematic liquid crystal cladding layer. An optimum design for achieving a large switching angle is presented. Experimental 2 X 2 matrix switches, which were fabricated on the basis of experimental results on the fundamental 1 X 2 switch, are demonstrated.

Manuscript received April 1, 1982; revised June 14, 1982.

The authors are with the Ibaraki Electrical Communication Laboratory, Nippon Telegraph and Telephone Public Corporation, Tokai, Ibaraki-ken, Japan.

0018-9480/82/1000-1591$00.75

II. 1 X 2 Elemental Waveguide Switch

A. Principle of Device Operation

Conventional devices using liquid crystal as a waveguide film have a disadvantage of large propagation loss, typically 20–37 dB/cm [11]-[13]. The propagation loss originates in scattering caused by the ordering fluctuation of liquid crystal molecules. To overcome this problem, liquid crystal is used as a cladding layer for a waveguide in the present switch. Since the power portion of propagating light penetrating into the lossy liquid crystal cladding layer is small and most power is confined in the waveguide film, propagation loss becomes lower than that for the conventional devices.

Fig. 1 shows the basic structure of the 1 X 2 liquid crystal waveguide switch formed in a slab waveguide. The switch consists of the Si substrate, which is used as a lower electrode, a SiO_2 buffer layer, SiO_2-Ta_2O_5 waveguide film [14], a SiO_2 surface treatment layer, a nematic liquid crystal layer, an upper surface treatment layer, and an upper electrode. The buffer layer is necessary to prevent propagating light leakage from the waveguide film into the substrate, caused by the fact that the refractive index of the substrate (e.g., 3.8 at 0.633 μm wavelength) is larger than that of the waveguide film (e.g., 1.76).

In order to support a guided mode in the waveguide film, the refractive index of each layer must be chosen to satisfy the condition $n_2 > (n_1, n_3, n_4)$, where n_1, n_2, n_3, n_4 are the refractive indexes of the buffer layer, waveguide film, surface treatment layer, and liquid crystal layer, respectively.

The function of the liquid crystal cladding layer will now be described. The rod-like shape of liquid crystal molecule leads to dielectric and optical anisotropies. The dielectric anisotropy is defined as $\Delta\epsilon = \epsilon_{\parallel} - \epsilon_{\perp}$, where $\epsilon_{\parallel}$ and $\epsilon_{\perp}$ are the dielectric constants parallel and perpendicular to the molecular long axis. The dielectric anisotropy can take both positive and negative values, depending on permanent dipole moment direction of the molecule. The optical anisotropy is defined as $\Delta n = n_e - n_o$, where n_e and n_o are refractive indexes parallel and perpendicular to the molecular long axis. The optical anisotropy Δn is always positive, i.e., $n_e > n_o$, since only the electron polarizability contributes to the refractive index in an optical frequency region. By using a suitable surface treatment layer, such as SiO_x oblique evaporated layer or a rubbed polymer layer, either the homogeneous state (molecular alignment parallel to the surface) or the homeotropic state (molecular alignment perpendicular to the surface) can be achieved depending on the dielectric anisotropy. When an electric field is applied across the liquid crystal, the molecules align themselves with the electric field. In the case of positive liquid crystal ($\Delta\epsilon > 0$), the initial homogeneous state changes to the homeotropic state by applying the electric field. On the other hand, for negative liquid crystal, the initial homeotropic state changes to the homogeneous state under the external electric field.

A TE (or TM) mode switch can be obtained by both the use of the positive (or negative) liquid crystal and the preparation of the initial homogeneous (or homeotropic) state. Here, let us consider a TE mode switch used in the experiments, shown in Fig. 1. The waveguide has two regions, region I without the upper electrode and region II with the electrode. In the absence of the electric field, i.e., the off state, molecule alignments in region I and II are maintained in the initial homogeneous state, as shown in Fig. 1(b). Since the optical electric field of the TE mode coincides with the molecular long axis, the TE mode light sees the extraordinary refractive index n_e in both regions. As a result, the input light passes straight through without switching. On the other hand, when the electric field is applied, molecular alignment in region II is changed from the homogeneous state to the homeotropic state, as shown in Fig. 1(c). In this process, refractive index n_4 in region II varies also from n_e to n_o, where $n_e > n_o$. Therefore, the field distribution of propagating light becomes different between regions I and II, as shown typically in Fig. 2. This

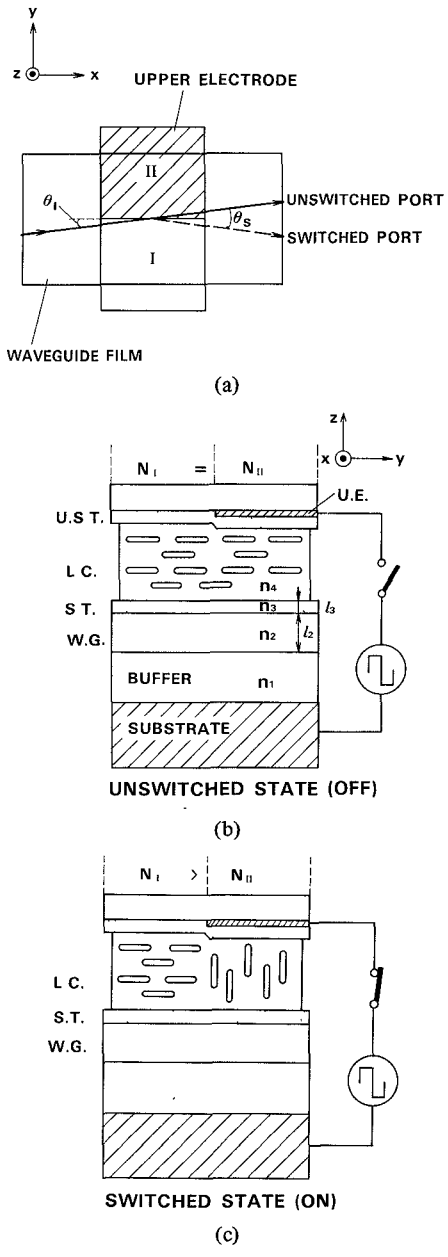

Fig. 1. Structure of the 1 X 2 optical waveguide switch using nematic liquid crystal: (a) top view, (b) and (c) are cross-sectional views of the switching off state and the on state, respectively. UE: upper electrode, UST: upper surface treatment layer, LC: liquid crystal layer, ST: surface treatment layer, WG: waveguide film.

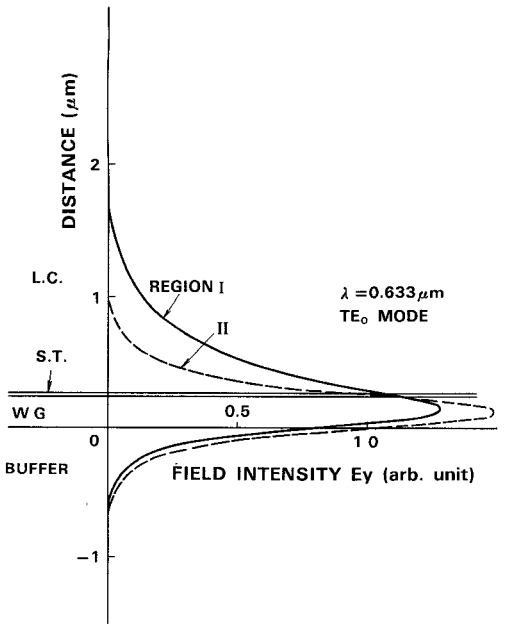

Fig. 2. Typical field distributions of propagating light in regions I and II. Field distributions were calculated for the experimental 1 × 2 switch.

field distribution difference means that effective refractive index N_{II} in region II is smaller than the index N_I in region I. Consequently, the input light is switched at the boundary between regions I and II by total internal reflection. However, input light angle θ_i must be smaller than the critical angle of total reflection θ_c which is defined as

$$\theta_c = \cos^{-1}(N_{II}/N_I). \tag{1}$$

B. Analysis of the Switching Angle

In order to fabricate the compact matrix switch and to obtain low crosstalk, it is necessary to make the switching angle as large as possible. The switching angle can be calculated using effective refractive index N. Let us assume a simplified four layer waveguide to examine the relation between the switching angle and the waveguide structure. The four layer waveguide is composed of a buffer layer with an infinite thickness, a waveguide film, a surface treatment layer, and a liquid crystal layer with an infinite thickness. Effective refractive index N is obtained by the following eigenvalue equation:

$$a_2 l_2 = \tan^{-1}(T_{21} a_1/a_2) - \tan^{-1}(T_{23}\phi a_3/a_2) + m\pi \tag{2}$$

where

$$a_i = k\sqrt{|N^2 - n_i^2|} \qquad (i = 1, 2, 3, 4)$$

$$T_{ij} = \begin{cases} 1 & \text{for TE mode} \\ (n_i/n_j)^2 & \text{for TM mode} \end{cases}$$

$$\phi = \frac{(a_3 - T_{34}a_4) - (T_{34}a_4 + a_3)\exp(2a_3 l_3)}{(a_3 - T_{34}a_4) + (T_{34}a_4 + a_3)\exp(2a_3 l_3)}$$

$$k = 2\pi/\lambda.$$

Here, m is the mode number, l_2 and l_3 are the thicknesses of waveguide film and surface treatment layer, respectively, and λ is the light wavelength in vacuum.

The maximum value of the switching angle θ_s between switched and unswitched lights is equal to twice the critical angle of total reflection θ_c, which is given by (1) and (2). In order to attain a large switching angle, conditions to obtain large critical angle θ_c must be considered. The critical angle θ_c depends on waveguide parameters, such as refractive indexes n_1-n_4 and layer thicknesses l_2 and l_3. Here, the discussion is concentrated on the relation between critical angle θ_c and the most important parameters for designing the switch such as the refractive index of the liquid crystal and the layer thicknesses of the waveguide film and the surface treatment layer. The material of each layer, except for the liquid crystal layer, was fixed on the experimental material. The refractive indexes n_1, n_2, and n_3 of the SiO_2 buffer layer, the SiO_2-Ta_2O_5 waveguide film, and the SiO_2 surface treatment layer are 1.461, 1.755, and 1.461, respectively, at 0.633 μm wavelength. Fig. 3 shows the critical angle θ_c dependence on extraordinary refractive index n_e, which is the refractive index of liquid crystal in the switching off state, with a parameter of waveguide film thickness l_2. Here, the surface treatment layer is supposed to be zero, i.e., $l_3 = 0$, to calculate the upper limiting value for the critical angle θ_c. The refractive index change Δn is fixed at 0.1. It can be seen from the figure that, under a given waveguide film thickness, the critical angle θ_c increases with an increase in refractive index n_e. The maximum critical angle θ_{cm} for each waveguide thickness is shown by the dashed line. Outside the dashed line is the cutoff area, where no guided mode exists in the waveguide film. The largest value of maximum critical angle θ_{cm} is a function of refractive index n_e and waveguide film thickness l_2. In this case, n_e of 1.58 and l_2 of 0.08 μm provide the largest critical angle of 16°. For a given refractive index n_e larger than that providing the largest θ_{cm}, critical angle θ_c increases with a decrease in waveguide film thickness l_2.

Fig. 4 shows the dependence of maximum critical angle θ_{cm} on refractive index n_e with a parameter of refractive index change $\Delta n = n_e - n_o$. Maximum critical angle θ_{cm} increases with an increase in Δn. In order to fabricate the switch, propagation loss must be taken into account, in addition to the conditions obtained from Figs. 2 and 3. Loss measurements of a SiO_2-Ta_2O_5 waveguide, composed of a Si substrate, a 1.4 μm SiO_2 buffer layer, SiO_2-Ta_2O_5 waveguide film, and air cladding, show that propagation loss increases with decreasing waveguide film thickness due to scattering loss at the waveguide surface roughness, and a film thickness of more than 0.2 μm is necessary to obtain a loss of less than 1.0 dB/cm. In a waveguide having liquid crystal cladding instead of air cladding, propagation loss increases much more. This film thickness limitation imposes a restriction on the available maximum critical angle. It can be seen from Fig. 4 that, under the condition of 0.2 μm waveguide film thickness, the available maximum critical angle ranges from 5.7 to 17.6°, corresponding to Δn of 0.1-0.2.

The critical angle in the case of the ideal switch having no surface treatment layer was discussed above. Here, the thickness effect of the surface treatment layer on critical angle θ_c is described. Fig. 5 shows critical angle θ_c dependence on waveguide thickness l_2 with a parameter of surface treatment

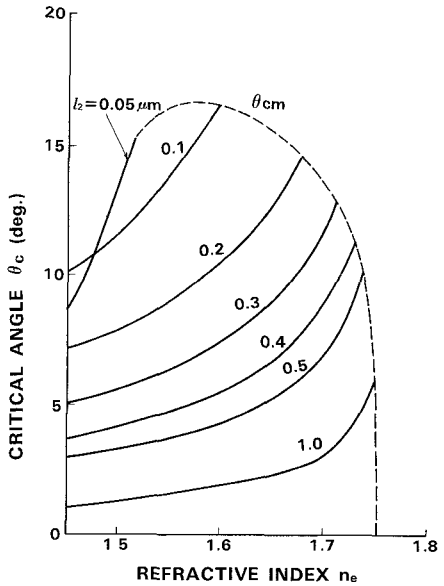

Fig. 3. Critical angle θ_C dependence on extraordinary refractive index n_e of liquid crystal with a parameter of waveguide film thickness l_2. Wavelength is 0.633 μm, surface treatment layer thickness is $l_3 = 0$, refractive index change is $\Delta n = n_e - n_o = 0.1$. The dashed line shows maximum critical angle θ_{cm}.

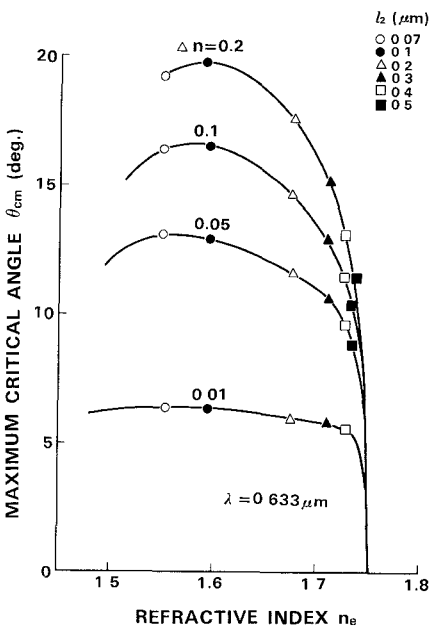

Fig. 4. Maximum critical angle θ_{cm} dependence on refractive index n_e with a parameter of refractive index change Δn. Wavelength = 0.633 μm, surface treatment layer thickness $l_3 = 0$.

layer thickness l_3. Nematic liquid crystal is assumed to be PCH1132 supplied by Merck, which was used in the present experiments. Its refractive indexes are $n_e = 1.629$ and $n_o = 1.501$ at the 0.633 μm wavelength. An increase in the surface treatment layer thickness results in a reduction in the critical angle θ_c. Since the critical angle θ_c is sensitive to surface treatment layer thickness l_3, precise thickness control of l_3 is needed.

From the analysis of critical angle θ_c, the following conditions are required for obtaining the large switching angle θ_s = (twice the critical angle θ_c).

1) Waveguide film thickness is as thin as possible in the thickness range given the permissible propagation loss.

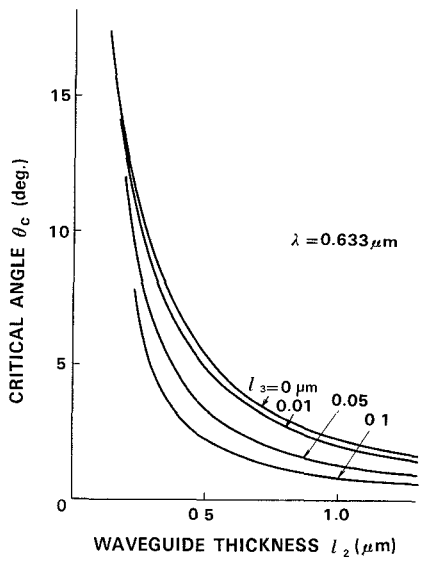

Fig. 5. Critical angle θ_C dependence on waveguide thickness l_2 with a parameter of surface treatment layer thickness l_3 at 0.633 μm wavelength. $n_e = 1.629, n_o = 1.501$.

2) For a given waveguide film thickness, the larger refractive index n_e of the liquid crystal layer is desirable.

3) Refractive index change Δn of the liquid crystal layer is as large as possible.

4) Surface treatment layer thickness is as thin as possible.

C. 1 × 2 Switch Experiment

The structure of an experimental 1 × 2 switch is the same as that shown in Fig. 1. Parameters of the switch for the TE_0 mode are summarized in Table I. Experiments were made with visible light of 0.633 μm wavelength (He-Ne laser) to visually observe switching action.

The switch parameters were determined by taking into consideration the conditions to obtain a large switching angle and commercially available liquid crystal materials. The SiO_2 buffer layer, 1.4 μm thick, and the SiO_2-Ta_2O_5 waveguide film, 0.25 μm thick, were successively deposited on Si substrate by sputtering. Propagation losses of the waveguide, without and with liquid crystal layer, were 0.8 and 2.1 dB/cm, respectively. The nematic liquid crystal used is PCH1132, supplied by Merck, whose chemical composition is a mixture of three phenylcyclohexane single components and one biphenylcyclohexane single substance, and which has a large positive dielectric anisotropy ($\Delta\epsilon = +10.3$). The liquid crystal layer thickness was adjusted to be about 9 μm by a polymer spacer. The SiO_2 surface treatment layer, 0.05 μm thick, was successfully made by an oblique evaporation technique. The rubbing method, which is usually used in liquid crystal display fabrication, was also tried to obtain liquid crystal alignment. Although molecular alignment was achieved by rubbing a surface treatment organic film coated on the waveguide film, this method was not applicable to the experimental switch because of the large propagation loss of more than 30 dB/cm. An In_2O_3 film was used as the upper transparent electrode.

Fig. 6 shows the switching action of the experimental switch. The light beam was coupled into the waveguide by the prism coupler method. Insertion losses at unswitched and switched ports are 5.7 and 9.8 dB, respectively. Crosstalks at unswitched

TABLE I
PARAMETERS OF 1 X 2 SWITCH OPERATED AT 0.633 μm WAVELENGTH

Layer	Material	Refractive index	Thickness (μm)
Substrate	Si wafer	3.8	—
Buffer	SiO_2	1.461	1.4
Waveguide film	SiO_2-Ta_2O_5(25mol%)	1.755	0.25
Surface treatment	SiO_2	1.461	0.05
Liquid crystal	Merck PCH 1132	n_e 1.629 n_o 1.501	9.0

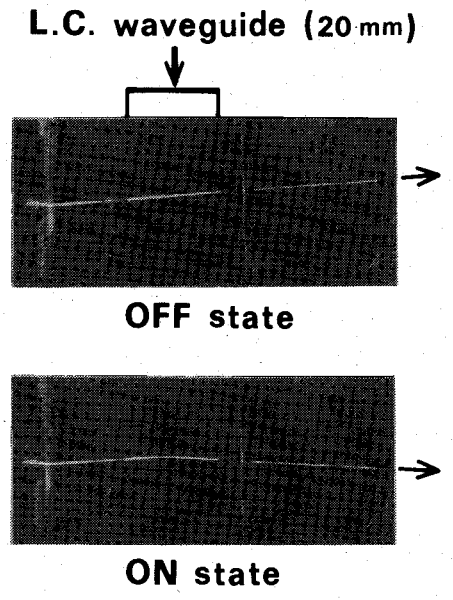

Fig. 6. Light streaks showing switching action of the experimental 1 X 2 switch at 0.633 μm wavelength.

and switched ports are -16.5 and -30.2 dB, respectively. Here, crosstalk is defined as 10 log (undesired light power/desired light power) in dB at any port. At the switched port, crosstalk is remarkably good, although the insertion loss is large. The insertion loss was mainly caused by scattering in the liquid crystal layer. The scattering bright light streak in the liquid crystal waveguide is clearly observed near the center of the waveguide in Fig. 6.

Fig. 7 shows output intensities at the unswitched and switched ports versus applied rms voltage (1 kHz square wave). Switching begins above 25 V. The switch is turned fully into the on state at 120 V.

A switched angle of 8.5° was obtained. The experimental switching angle is larger than that of less than 4° in the conventional $LiNbO_3$ total reflection matrix switch. However, the experimental value is relatively small compared with the predicted value of 16.6° from Fig. 5. Anticipated major reasons for the small switching angle are as follows. 1) An unchanged homogeneous boundary layer is left near the waveguide surface, even under large external electric field, where liquid crystal molecules cannot rotate due to the so-called "wall effect" of the surface treatment layer. 2) The initial refractive index of the liquid crystal layer is smaller than the value of n_e obtained in a bulk liquid crystal because the molecular long axes in the initial homogeneous state tilt to the surface treatment layer by typically 20-30°, due to an alignment property of the oblique evaporated SiO_2 film. The contribution of reason 2) to the critical angle is estimated to

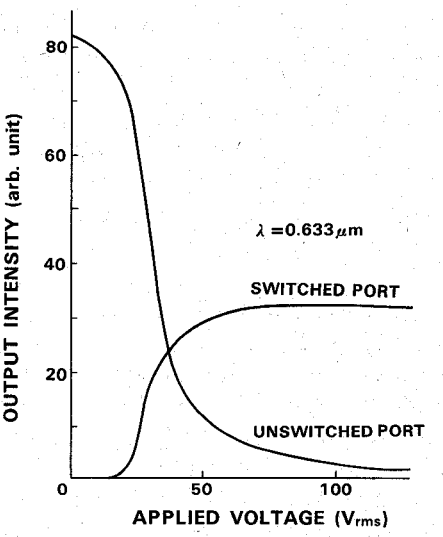

Fig. 7. Output intensities at unswitched and switched ports versus applied voltage in 1 X 2 switch.

be a decrease in the critical angle by at most 0.7°, even provided that the tilting angle is 30°. When reason 1) is considered, the switching angle should be analyzed based on a five layer waveguide (Appendix). In the five layer waveguide, the liquid crystal layer is divided into two layers, which are the main layer with changeable refractive index and a boundary layer with an unchanged refractive index. The estimated thickness of the boundary layer is 0.20 μm. The estimated thickness is in agreement with the reported value of 0.2-0.3 μm in [15], [16]. The estimated value is applicable to designing the switching angle, as will be described later.

Since it is difficult to reduce the thickness of the liquid crystal boundary layer, switching angle improvement by means of a reduction in the surface treatment layer thickness was studied to fabricate the compact matrix switch. In the second 1 X 2 experimental switch, in which the surface treatment layer thickness was reduced to 0.01 μm, an improved switching angle of 12° was obtained. Insertion losses at unswitched and switched ports are 15.9 and 20.7 dB, respectively. Crosstalks at unswitched and switched ports are -19.7 and -17.8 dB, respectively. Insertion losses in the second 1 X 2 switch are relatively large in comparison with 5.7-9.8 dB loss of the first 1 X 2 switch with 0.05 μm thick surface treatment layer. This is considered to arise from the fact that the light field penetration into the lossy liquid crystal layer becomes deeper through the use of the thin surface treatment layer. The increased scattering loss will lead to the degradation of crosstalk from -30.2 dB in the first 1 X 2 switch to -17.8 dB in the second 1 X 2 switch.

III. 2 X 2 NONBLOCKING MATRIX SWITCH

The switching angle of 12°, obtained in the second 1 X 2 experimental switch, was sufficient to construct a matrix switch. However, the large insertion loss was a problem to be solved. Recently, it was shown that the scattering loss for liquid crystal filled in a glass capillary decreases inversely in proportion to the square of light wavelength, and that the PCH liquid crystal has low absorption loss windows at the 1.3 and 1.55 μm wavelengths, which coincide with low propagation loss regions of optical fiber [17]. The slab waveguide 2 X 2 matrix switch, for 1.31 μm wavelength operation,

which makes positive use of the interesting properties of the liquid crystal, was fabricated. Switch parameters are listed in Table II.

The present liquid crystal switch has an advantage in that the matrix switch can be fabricated by only preparing a patterned upper electrode. Fig. 8 shows the experimental patterned electrode and four switching points. I_1 and I_2 are input ports and O_1 and O_2 are output ports. The distance between input ports I_1 and I_2 is 1 mm, and that between output ports O_1 and O_2 is also 1 mm. Ports M_1 and M_2 are used as monitoring ports, not output ports because crosstalks at ports M_1 and M_2 are worse than at output ports O_1 and O_2 due to the fact that light leaks caused by imperfect switching action at the switching points reach ports M_1 and M_2. The matrix size, including four switching points, is 5 X 20 mm.

Fig. 9 shows the critical angle θ_c dependence on waveguide film thickness l_2 with a parameter of liquid crystal boundary layer thickness l_4. Calculation of θ_c was made based on the five layer waveguide model. It can be seen that a switch having a 0.5 μm waveguide film and a liquid crystal boundary layer with 0.20 μm thickness, which is the estimated value from the first 1 X 2 switch experiment, provides the switching angle of 13.6° (twice the critical angle of 6.8°). The experimental switching angle was 14° in the 2 X 2 switch. The experimental and theoretical values are in good agreement. The switching characteristics are summarized in Table III. Measurements were made using an LNP ($LiNdP_4O_{12}$) laser pumped by an Ar laser [18]. The laser beam with 2.5 mm diameter was focused to a beam spot with 0.4 mm diameter and was introduced into the waveguide film by the prism coupler. Although crosstalks were almost the same as for the second 1 X 2 switch for 0.633 μm wavelength operation, insertion losses were reduced from 20.7 to 7.7 dB. Estimated propagation loss in the liquid crystal waveguide is 2.3 dB/cm. Operation at the 1.3 μm wavelength was very effective in reducing insertion loss, as expected. Fig. 10 shows the characteristic of the switching point S_{11}. The characteristics of the other switching points S_{12}, S_{21}, and S_{22} were almost the same as that of the switching point S_{11}. A driving voltage of 30 V_{rms} (1 kHz square wave) is sufficient for switching action. The switching rise time and fall time were 2 and 4 ms, respectively.

In order to put this type of the waveguide switch to practical use, the problem of coupling between the switch and single-mode fibers must be solved. It is difficult to use the end-fire coupling method because the waveguide film thickness of 0.5 μm in the present switch is fairly thin compared with the fiber core diameter of a few micrometers. Although the prism coupler was used in the experiment, it has the disadvantages of mechanical instability, large size, and difficulty in fixing the fibers on the prisms. The modified prism coupler with rigid structure is under study.

IV. Conclusion

Electrically controlled waveguide optical switches using nematic liquid crystal were demonstrated to have a potential for application to a nonblocking matrix switch. A 2 X 2 nonblocking matrix switch composed of four switching points for 1.31 μm wavelength operation showed 7.3-7.7 dB insertion

TABLE II
Parameters of 2 X 2 Matrix Switch for 1.31 μm Wavelength

Layer	Material	Refractive index	Thickness (μm)
Substrate	Si wafer	3.4	—
Buffer	SiO_2	1.450	2.1
Waveguide film	SiO_2-Ta_2O_5(25mol%)	1.741	0.50
Surface treatment	SiO_2	1.450	0.01
Liquid crystal	Merck PCH 1132	n_e 1.609 n_o 1.492	9.0

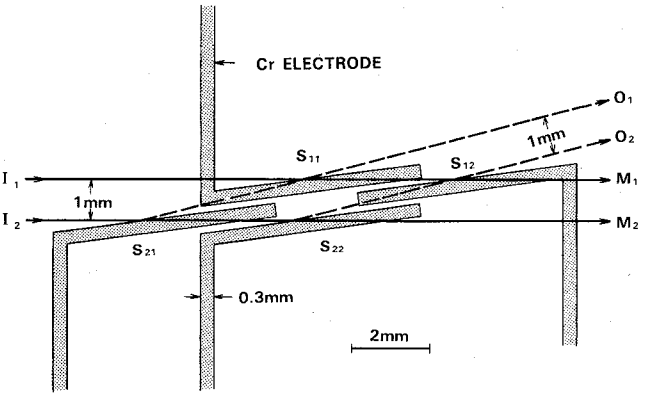

Fig. 8. Patterned upper electrode including four switching points ($S_{11}, S_{12}, S_{21}, S_{22}$) for 2 X 2 matrix switch.

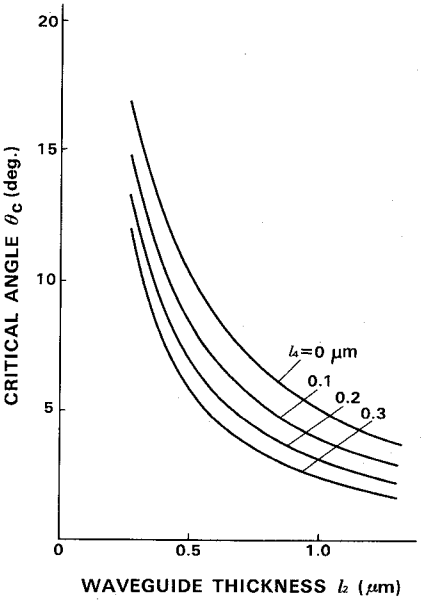

Fig. 9. Critical angle θ_c dependence on waveguide film thickness l_2 with a parameter of liquid crystal boundary layer thickness l_4 at 1.31 μm wavelength.

TABLE III
Characteristics of 2 X 2 Matrix Switch for 1.31 μm Wavelength Operation

Port	Insertion loss (dB)	Crosstalk (dB)
M_1	6.2	−10.0
M_2	6.1	−8.6
O_1	7.3	−17.3
O_2	7.7	−18.2

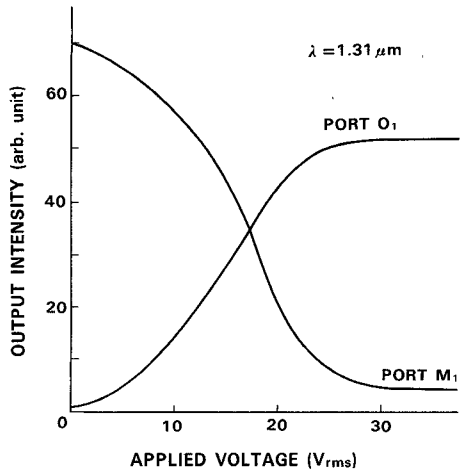

Fig. 10. Characteristic of the switching point S_{11} in 2 × 2 matrix switch for 1.31 μm wavelength operation.

loss and −17.3 to −18.2 dB crosstalk. Long wavelenth operation of 1.3 μm was effective in reduction in the insertion loss caused by liquid-crystal scattering. It was found that the switching angle can be designed based on a five layer waveguide composed of a buffer layer, a waveguide film, a surface treatment layer, a liquid crystal boundary layer with unchanged refractive index, and a liquid crystal main layer with changeable refractive index.

The features of the liquid crystal waveguide switch are as follows:

1) large switching angle of 14° which makes matrix switch fabrication easy;

2) easy matrix switch fabrication because it requires only a patterned upper electrode;

3) low propagation loss of 2.3 dB/cm compared with that of more than 20 dB/cm in conventional devices with liquid crystal waveguide film; and

4) nonblocking switch having no mechanically moving parts.

Appendix

In case the liquid crystal layer is divided into two layers, the effective refractive index N for the TE_0 mode is calculated from the following eigenvalue equation. The waveguide consists of a buffer layer (refractive index n_1), waveguide film (n_2), surface treatment layer (n_3), liquid crystal boundary layer (n_4), and liquid crystal main layer (n_5). Here, $n_2 > n_4 > n_5 > (n_1, n_3)$. The thicknesses of the buffer layer and the liquid crystal layer are assumed to be infinite, and those of the waveguide layer, surface treatment layer, and the liquid crystal boundary layer are l_2, l_3, and l_4, respectively.

For $n_2 > N > n_4$,

$$\{(a_3 - a_4)(a_4 - a_5)\exp(-2a_4l_4) + (a_3 + a_4)(a_4 + a_5)\}$$
$$\cdot \{(a_1a_2 + a_2a_3) + (a_1a_3 - a_2^2)\tan a_2l_2\}$$
$$- \exp(-2a_3l_3)\{(a_3 + a_4)(a_4 - a_5)\exp(-2a_4l_4)$$
$$+ (a_3 - a_4)(a_4 + a_5)\} \cdot \{a_2(a_3 - a_1) + (a_1a_3 + a_2^2)$$
$$\cdot \tan a_2l_2\} = 0.$$

For $n_4 > N > n_5$,

$$\{a_2(a_1 + a_3) + (a_1a_3 - a_2^2)\tan a_2l_2\}$$
$$\cdot \{a_4(a_3 + a_5) + (a_3a_5 - a_4^2)\tan a_4l_4\}$$
$$- \exp(-2a_3l_3)\{a_4(a_3 - a_5) + (a_3a_5 + a_4^2)\tan a_4l_4\}$$
$$\cdot \{a_2(a_3 - a_1) + (a_1a_3 + a_2^2)\tan a_2l_2\} = 0$$

where

$$a_i = k\sqrt{|N^2 - n_i^2|} \quad (i = 1 \sim 5).$$

Acknowledgment

The authors wish to thank K. Matsuyama, H. Takata, T. Manabe, and T. Edahiro for their encouragement and helpful discussions.

References

[1] H. Yamamoto, M. Yokoyama, H. Ogiwara, and M. Yoshida, "Large-scale and low-loss optical switch matrix for optical switching systems," *J. Opt. Commun.*, vol. 1, pp. 74–79, 1980.

[2] J. Minowa, Y. Fujii, Y. Nagata, and K. Doi, "Nonblocking 8 × 8 optical matrix switch for fiber-optic communication," *Electron. Lett.*, vol. 16, pp. 422–423, May 1980.

[3] H. Terui, M. Kobayashi, and J. Noda, "2 × 2 optical waveguide matrix switch using dielectric chip motion," *Appl. Opt.*, vol. 21, pp. 1979–1984, June 1982.

[4] R. A. Soref and D. H. McMahon, "Multimode 2 × 2 optical crossbar switch," *Electron. Lett.*, vol. 14, pp. 283–284, Apr. 1978.

[5] R. A. Soref, "Multimode 3 × 2 fiber optical matrix switch," in *Fiber Optics–Advances in R&D*, B. Bendow and S. S. Mitra Eds. New York: Plenum, 1979.

[6] R. A. Becker and W.S.C. Chang, "Electrooptical switching in thin film waveguides for a computer communication bus," *Appl. Opt.*, vol. 18, pp. 3296–3300, Oct. 1979.

[7] C. L. Chang and C. S. Tsai, "GHz bandwidth optical channel waveguide TIR switches and 4 × 4 switching networks," in *Tech. Dig. Top. Meet. on Integrated and Guided-Wave Optics*, Jan. 1982, paper THD2.

[8] R. V. Schmidt and L. L. Buhl, "Experimental 4 × 4 optical switching network," *Electron. Lett.*, vol. 12, pp. 575–577, Oct. 1976.

[9] R. A. Soref, "Electrooptic 4 × 4 matrix switch for multimode fiber-optic systems," *Appl. Opt.*, vol. 21, pp. 1386–1393, Apr. 1982.

[10] J. P. Sheridan, J. M. Schnur, and T. G. Giallorenzi, "Electro-optic switching in low-loss liquid crystal waveguides," *Appl. Phys. Lett.*, vol. 22, pp. 560–561, June 1973.

[11] C. Hu and J. R. Whinnery, "Losses of a nematic liquid-crystal electrooptic devices," *Appl. Opt.*, vol. 12, pp. 2309–2311, Oct. 1973.

[12] T. G. Giallorenzi and J. P. Sheridan, "Light scattering from nematic liquid crystal waveguides," *J. Appl. Phys.*, vol. 46, pp. 1271–1282, Mar. 1975.

[13] J. R. Whinnery, C. Hu, and Y. S. Kwon, "Liquid-crystal waveguides for integrated optics," *IEEE J. Quantum Electron.*, vol. QE-13, pp. 262–267, Apr. 1977.

[14] H. Terui and M. Kobayashi, "Refractive-index-adjustable SiO_2-Ta_2O_5 films for integrated optical circuits," *Appl. Phys. Lett.*, vol. 32, pp. 666–668, May 1978.

[15] R. A. Kashnow and C. R. Stein, "Total-reflection liquid crystal electrooptic devices," *Appl. Opt.*, vol. 12, pp. 2309–2311, Oct. 1973.

[16] R. A. Soref and D. H. McMahon, "Total switching of unpolarized fiber light with a four-port electrooptic liquid-crystal device," *Opt. Lett.*, vol. 5, pp. 147–149, 1980.

[17] M. Kawachi, N. Shibata, and T. Edahiro, "Possibility of liquid crystal as optical waveguide material for 1.3 μm and 1.5 μm bands," *Japan. J. Appl. Phys.*, vol. 21, pp. L162–L164, Mar. 1982.

[18] K. Kubodera, K. Otsuka, and S. Miyazawa, "Stable $LiNdP_4O_{12}$ miniature laser," *Appl. Opt.*, vol. 18, pp. 884–890, Mar. 1979.

Morio Kobayashi was born in Nagano, Japan, on March 31, 1943. He received the B.S. degree from the Science University of Tokyo, Japan, in 1967, and the M.S. degree from Osaka City University, Osaka, Japan, in 1969.

In 1969 he joined Musashino Electrical Communication Laboratory, and in 1971 he joined the Ibaraki Electrical Communication Laboratory, Nippon Telegraph and Telephone Public Corporation, Ibaraki-ken, Japan. He was initially engaged in the research of electrophotography. He is presently engaged in research on optical guided-wave devices.

Mr. Kobayashi is a member of the Institute of Electronics and Communication Engineers of Japan and the Japan Society of Applied Physics.

Hiroshi Terui was born in Aomori, Japan, on February 18, 1950. He received the B.S. and M.S. degrees in physics from Tohoku University, Japan, in 1972 and 1974, respectively.

In 1974 he joined the Ibaraki Electrical Communication Laboratory, Nippon Telegraph and Telephone Public Corporation, Ibaraki-ken, Japan, where he was engaged in research on materials for magnetooptic recording. Since 1976 he has been engaged in research on optical guided-wave devices.

Mr. Terui is a member of the Institute of Electronics and Communication Engineers of Japan and the Japan Society of Applied Physics.

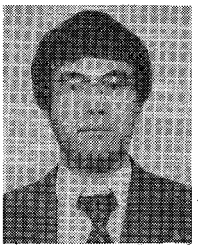

Masao Kawachi was born in Gunma, Japan, on March 17, 1949. He received the B.S. and M.S. degrees in physical electronics and the Ph.D. degree from Tokyo Institute of Technology, Tokyo, Japan, in 1971, 1973, and 1978, respectively.

In 1973 he joined the Ibaraki Electrical Communication Laboratory, Nippon Telegraph and Telephone Public Corporation, Ibaraki-ken, Japan, where he was engaged in research on liquid crystals and their application to display devices. He is presently engaged in research on optical fiber fabrication and integrated optical devices.

Dr. Kawachi is a member of the Institute of Electronics and Communication Engineers of Japan and the Japan Society of Applied Physics.

Juichi Noda, for a biography, see this issue, p. 1560.

Guided Wave Approaches to Optical Bistability

GEORGE I. STEGEMAN, MEMBER, IEEE

Abstract—**We have analyzed four different guided wave approaches to achieving a power dependent refractive index and optical bistability. These include surface plasmons at the interface between a metal and a semiconductor, symmetric surface plasmon modes guided by thin metal films, conventional single film integrated optics waveguides, and multifilm integrated optics. The relative merits of each geometry are discussed for utilizing the large cubic nonlinearities in the semiconductors GaAs and InSb. Both the mode attenuation and the minimum power required for a nonlinear phase shift of $\pi/2$ are evaluated numerically and it is shown that usable propagation distances can be obtained, even for highly lossy media such as GaAs.**

I. Introduction

THE phenomenon of optical bistability [1]-[3] has generated a great deal of interest in potential applications [4]-[6]. It occurs when a medium with an intensity dependent refractive index is placed within a resonator structure with the result that both the power reflected from and transmitted through the device are no longer linear with incident power. This can lead to two states and switching between them, regions of optical gain, etc. Devices based on this phenomenon require materials with large third order nonlinearities, interaction geometries characterized by high optical power densities and long enough propagation distances to produce useful nonlinear phase shifts, and optical resonators. With the exception of a few hybrid integrated optics devices [7]-[11] most experiments reported to date have been performed in bulk media, frequently near the focal length of a lens (to produce the necessary high power densities).

Optical waves guided by single or multiple interfaces offer an attractive approach to producing high power densities over the long propagation distances desirable for optically bistable devices based on intrinsic (material) nonlinearities. For the practical realization of such devices, there are three important factors to be considered. First, the propagation distance over which bistability is achieved should be maximized. In terms of a single device, distances $\geqslant 10^3$ optical wavelengths are desirable to facilitate coupling, etc. This is also an important consideration for stacking multiple devices into logic arrays, etc. Second, the power required for device operation should be a minimum for power dissipation and device density reasons. The minimum power is usually defined in terms of the total nonlinearly produced phase change required for a particular application; this value is usually less than $\pi/2$, which we shall adopt here as an upper limit. Third, a feedback mechanism compatible with guided wave technology is required. Distributed feedback via surface or volume gratings

Manuscript received March 4, 1982; revised May 17, 1982. This work was supported by the Office of Army Research and the Air Force Office of Scientific Research.

The author is with the Optical Sciences Center, University of Arizona, Tucson, AZ 85721.

0018-9480/82/1000-1598$00.75